Kinetics of relaxation and recombination of nonequilibrium carriers in GaAs: Carrier capture by impurities

D. Bimberg
Institut für Festkörperphysik I, Technische Universität Berlin, Strasse des 17 Juni 135, D-1000 Berlin 12, Germany

H. Münzel
Institut für Halbleitertechnik, Technische Hochschule Darmstadt, Schlossgartenstrasse 8, D-6100 Darmstadt, Germany

A. Steckenborn
Heinrich-Hertz-Institut für Nachrichtentechnik Berlin GmbH, Einsteinufer 37, D-1000 Berlin 10, Germany

J. Christen
Institut für Festkörperphysik I, Technische Universität Berlin, Strasse des 17 Juni 135, D-1000 Berlin 12, Germany
(Received 1 February 1985)

The kinetics of relaxation and recombination processes of nonequilibrium and quasiequilibrium charge carriers in high-purity *n*- and *p*-type GaAs are investigated. Luminescence spectra taken in time windows positioned at the end of excitation pulses of increasing length and the shape of corresponding luminescence transients are found to depend strongly on pulse length up to 500 ns. It is thus shown that quasiequilibrium of the excited state under continuous excitation is reached only after relatively long times. Slow capture of minority charge carriers by ionized impurities is found to cause the delay. Capture cross sections of holes by the ionized effective-mass acceptor carbon C^- and the ionized 167-meV deep Sn^- acceptor are determined from the onset of the respective luminescence in *n*-type samples. Time-delayed spectra and luminescence transients taken after the end of an exciting pulse of 2 μs length visualize the stepwise relaxation of the electronic system from the nonthermal quasiequilibrium of an excited state to thermal equilibrium. In all *n- and p*-type samples investigated here free holes disappear first. Consequently, the conductivity type of *p*-type material inverts twice during recombination. Capture cross sections of free electrons by ionized donors and neutral acceptors and of free holes by ionized carbon acceptors are determined. The capture cross sections are $\sigma(h\rightarrow Sn_{As}^-)=7.0\times10^{-13}$ cm^2, $\sigma(h\rightarrow C^-)=8.7\times10^{-14}$ cm^2, $\sigma(e\rightarrow D^+)=5.1\times10^{-15}$ cm^2, and $\sigma(e\rightarrow C^0)=2\times10^{-16}$ cm^2. A specially devised low-temperature cathodoluminescence system is used for these experiments. Electron pulses of varying length 1 ns$\leq t\leq$10 μs but constant rise and decay time of $\leq$200 ps and moderate to low power density ($0.8\leq I_{exc}\leq20$ W cm^{-2}) are employed for excitation.

I. INTRODUCTION

The thermal equilibrium number and distribution of charge carriers in a semiconductor is disturbed by injection or excitation. Band and impurity states which were empty before are now populated. The equilibrium is reestablished by relaxation, capture, and recombination of the charge carriers.

In this paper we present a detailed analysis of the kinetics of the various capture and recombination processes reestablishing the *thermal equilibrium number of charge carriers* in GaAs at low temperatures. GaAs, whose electronic properties are now well understood, is *the ideal model substance* for the entire class of direct-band-gap zinc-blende semiconductors. In a subsequent paper we will treat the energy relaxation of warm carriers in their respective bands via acoustic-phonon emission.

The "lifetimes" of nonequilibrium electrons and holes in their different band and impurity states are of central interest, both from a fundamental and an applied point of view. Capture cross sections can be derived from lifetimes. Properties and performance limits of many devices depend on capture cross sections: The speed of electronic switches, the response time of ir-radiation detectors, and the efficiency of solar cells and lasers are among the most important properties.

Since the advent of semiconductor physics considerable effort has been devoted to calculate cross sections of transitions between bands and impurities. This problem shows a varying degree of complexity, depending on the type of impurity (effective-mass type or deep) and the type of transition (involving an impurity state derived from the same or a different band) considered. In particular, a lack of knowledge of the proper impurity wave function often presents a major source of difficulty.

Pioneering work was performed by Bebb and Chapman,[1] who borrowed the phenomenological quantum-defect method (QDM) from atomic physics and applied it to the case of impurities with a Coulomb potential plus a short-range potential. The δ-function model for very deep

centers was developed by Lucovsky.[2] Very shallow centers are described in the framework of hydrogenic effective-mass theory. In the special case in which the number of core electrons of the impurity is identical to that of the host, a single-band approximation of the impurity wave function is valid regardless of whether it is shallow or deep. An up-to-date review of the validity of the effective-mass theory and on isocoric impurities has been given by Pantelides.[3] Bebb[4] used the QD wave functions to calculate the optical-transition cross sections involving an impurity. Ridley[5] derived approximate analytical expressions for photoionization cross sections and their temperature dependence. In contrast to earlier work, contributions of Bloch functions from *many* bands to the localized state were considered. Very recently, in an excellent paper, Chaudhuri[6] pointed out a number of important deficiencies of the earlier work. By eliminating unjustified approximations, correcting errors, and using a novel method to compare the overlap integrals of the cell periodic functions, Chaudhuri derived a rather general formalism to calculate for the first time the zero-temperature cross sections for *both* types of transitions: band-impurity transitions and photoionization or photodeionization. As an example and application of his method, he chose GaAs. Unfortunately, the complexity which arises due to the degeneracy of the valence band in zinc-blende semiconductors was not taken into account, although it is known that neither correct acceptor energy levels[7,8] nor their shift and splitting in external magnetic fields[9] can be obtained with simple effective-mass theory. Thus a quantitative comparison of the numerical results for transition cross sections[6] involving acceptors, e.g., in GaAs, to experimental values is hampered. It is, however, correctly argued[6] that there exist no experimental data for band-acceptor transitions and comparison, anyway, cannot yet be made. This situation is altered with the present work, where—to the best of our knowledge—for the first time cross sections of conduction-band–acceptor transitions, of hole capture by the ionized effective mass acceptor carbon[9] and by the ionized 167-meV deep acceptor tin,[10] and of electron capture by ionized donors are presented.

There exist a number of standard methods for the experimental determination of capture (or emission) cross sections of impurities and defects. Deep-level transient spectroscopy[11] (DLTS) and various other capacitance spectroscopic methods[12] were developed and brought to a high standard with cross-section determination as one of the main aims. Frequently, however, a substantial variation of the rates and therefore the cross sections with the magnitude of the externally applied electric field (e.g., of the Schottky barrier) is observed.[13] An unambiguous assertion on the zero-field cross section is hampered. Furthermore, it is technically difficult to determine cross sections of shallow impurities by DLTS, and, to our knowledge, there exist no data, e.g., on cross sections of transitions from the neighboring or the opposite band to effective-mass acceptors or donors in GaAs.[14] Cross sections are more sensitive to the proper choice of wave function and to the correct choice of approximations very often made in the course of theoretical work than energies. Experimental data on effective-mass acceptors, moderately deep acceptors, and effective-mass donors—presented here for the first time—thus provide a key to test the validity of fundamental theoretical work.[6–8]

Time-resolved luminescence experiments represent the most important and most powerful optical tool to gain information on lifetimes. Different capture processes can be distinguished by separate measurement of the transient behavior of the various lines and bands of a luminescence spectrum. Complementary information is obtained by separate observation of the onset and the decay of the luminescence.

The importance and the large number of applications of time-resolved luminescence present a challenge to experimenters to develop sources of excitation, detection, and data-acquisition systems. The work of Heim[15] reviews those methods having a time resolution in the domain between 10^{-9} and 10^{-6} s. Common to all of them is the use of various types of pulsed lasers as excitation sources. The width of such a laser pulse cannot be independently adjusted from its rise and decay time and presents a limit for the time resolution of the system. Until now the question was never considered of whether the shape of the exciting laser pulses does not directly affect the luminescence transients and all quantities derived from it. One reason why one might have doubts are the relatively long capture times of free charge carriers into shallow impurities in both direct- and indirect-band-gap semiconductors, which can be estimated on the basis of the above-mentioned,[6] and additional, theoretical work:[16–18] capture times long enough to prevent a *metastable* excited state being established in the semiconductor during excitation. If such a state is not reached, the initial state of the decay is completely undefined, depending on small details of the exciting pulse shape, and any interpretation of results is questionable. No reports of time-resolved luminescence experiments assessing systematically the influence of a source of excitation with variable length and intensity, but constant and extremely short decay time exist to date.

In this paper a different approach to performing time-resolved luminescence experiments is presented, utilizing a source of excitation circumventing the drawbacks of a classical laser source: a chopped cathode ray. Pulses of electrons with constant rise and decay times of $\leq$200 ps and continuously variable lengths between $\leq$1 ns and 10 μs are created in a scanning electron microscope equipped with a beam-blanking unit, a miniaturized He cryostat, and a cathodoluminescence detection system using a special photon-counting technique. High-purity *n*- and *p*-type GaAs is investigated. Luminescence *spectra* and *transients* are measured *as a function of increasing pulse length* (keeping all other parameters constant) and are indeed found to vary strongly for lengths up to 1 μs! Hole and electron capture times and cross sections into states of ionized acceptors and donors, respectively, are derived from these "luminescence onset" data.

Subsequently, the *decay* from a *metastable* excited state is investigated as a function of excitation intensity, temperature, and doping using pulses of some μs length. A detailed analysis of these data allows a conclusive inter-

pretation of the underlying, very complex recombination kinetics, and an additional determination of cross sections to be compared with the values based on the luminescence onset.

Surprisingly, we observe that holes always disappear before free electrons disappear, independent of the type of sample, due to the much larger capture cross section of free holes. Thus, strongly excited p-type samples change conductivity type for a short time during decay.

This paper is organized as follows: Section II contains a description of the experimental setup and of the samples used. In Sec. III results of experiments with variable pulse lengths are presented. Time-delayed spectra and decay times from a quasiequilibrium excited state, reached after a long excitation pulse is abruptly switched off, are presented and discussed in Sec. IV. Concluding remarks are found in Sec. V.

II. EXPERIMENTAL SETUP AND PROCEDURES

This section contains a description of the low-temperature cathodoluminescence system. A detailed account emphasizing its potential for the generation of luminescence intensity and lifetime *pattern* of semiconductor surfaces and structures has been given elsewhere.[19] At the end of this section some properties of the samples used for our experiments are summarized.

A. Setup for time-resolved cathodluminescence experiments

The cathodoluminescence (CL) system—a block diagram is shown in Fig. 1—is based on a commercial scanning electron microscope (SEM). The vacuum system is modified and cryogenic shielding is introduced to suppress contamination of the samples at low temperatures.[20] A Raith beam-blanking unit is located directly below the electron gun. Electron pulses of rise and decay time ≤ 200 ps, varying width of ≤ 1 ns up to 10 μs, and a repetition rate of 1 kHz up to 1 MHz are used for excitation. A miniaturized continuous-flow He cryostat (Cryovac, Inc.) is fitted to a standard specimen stage. The temperature is continuously variable in the range $5 \leq T \leq 300$ K. Lattice, charge-carrier, and exciton temperatures of typical samples are determined independently as described earlier[20,21] to control or avoid heating of the lattice relative to the cryostat. 30-keV electrons at varying currents yielding intensities $0.8 \leq I_{\text{exc}} \leq 20$ W/cm^2 are used for excitation in the work described here. At 30 keV the center of excitation is ≈ 1 μm below the surface. Surface effects can thus be excluded as contributing appreciably to the recombination.[22] The emitted light is focused by an elliptical mirror on to the entrance slit of a McPherson 30-cm vacuum monochromator (spectral resolution 0.06 nm at 10 μm slit width). The electron beam is always scanned over a small square of 7×7 μm^2 and the luminescence light presents a mean value of the properties of this area. The light is detected by a cooled photomultiplier with a GaAs cathode. A block diagram of the signal detection and regeneration system is shown in Fig. 2. The pulse

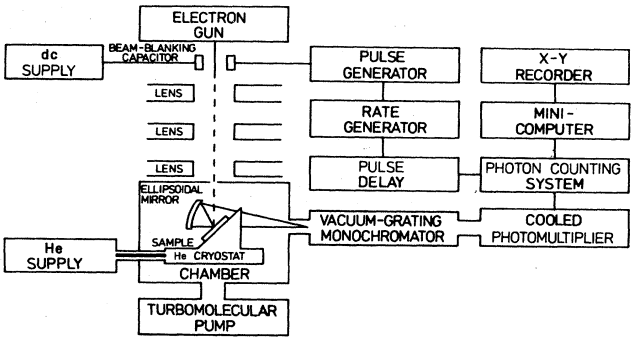

FIG. 1. Schematic diagram of the low-temperature cathodoluminescence setup attached to a scanning electron microscope. Temperature of the sample, $5 \leq T \leq 300$ K. Time resolution of the system, ≤ 250 ps.

generator which triggers the beam-blanking unit also triggers a photon-counting system via a delay line. The photon-counting system operates according to the method of delayed coincidence in an inverted mode, however, thus yielding an improved signal-to-noise ratio . The dynamic range of our detection system is $\cong 10^5$. The pulse-height distribution generated by the photon-counting system is evaluated by a computer-controlled (Digital Equipment Corporation LSI-11/23 minicomputer) multichannel analyzer (PGT), a system usually employed for energy-dispersive x-ray analysis. The data are stored on a magnetic disk. Our data-acquisition technique has the unique advantage that simultaneously up to 14 time windows

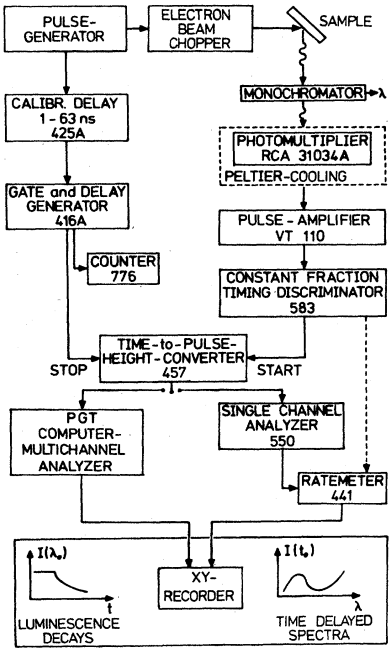

FIG. 2. Block diagram of electron-beam-blanking and cathodoluminescence detection system including a photon-counting system operating in an inverted mode and an LSI-11/23-minicomputer—controlled multichannel analyzer.

with varying widths—to optimize independently the signal-to-noise ratio—can be electronically set. Thus up to 14 spectra taken at different times with respect to the start of the exciting pulse can be recorded simultaneously under the same experimental conditions. No repetitive wavelength scans are necessary. The data-acquisition time is largely reduced as compared to a sequential measurement. The time resolution of the *total* CL setup including photomultiplier and electronics is experimentally determined to be $\leqq 250$ ps.

Figure 3 presents an illustration of this novel procedure. A 800-ns electron pulse is employed here to excite the luminescence. The onset of the luminescence and its kinetics, the quasisteady state, and the decay and its kinetics are seen.

Beyond the advantages already mentioned, a time-resolved cathodoluminescence experiment as described here is superior to a typical time-resolved photoluminescence experiment having similar time resolution from three more general points of view:

(a) The depth of excitation can be easily varied by varying the electron acceleration voltage between 200 V and 40 kV. The projected range of such electrons, e.g., in GaAs, varies from only a few nm to 5.3 μm, respectively. Thus, predominantly surface or surface-free excitation, respectively, can be chosen, depending on the requirements of the actual experiments. At any penetration depth the excitation is much more homogeneous in volume than after laser illumination.

(b) The width of the exciting pulses can be varied by more than 4 orders of magnitude without altering the pulse rise and decay time. Thus the temporal resolution of the experiment is independent of the pulse width.

(c) The electron beam can be easily scanned over the surface of the crystal using the standard scanning coils of the SEM. A two-dimensional pattern of the luminescence intensity and lifetime can be taken in a few minutes.[19]

A general remark shall conclude this section. A "straightforward" interpretation of the time dependence of the luminescence intensity—the "lifetime"—is dubious

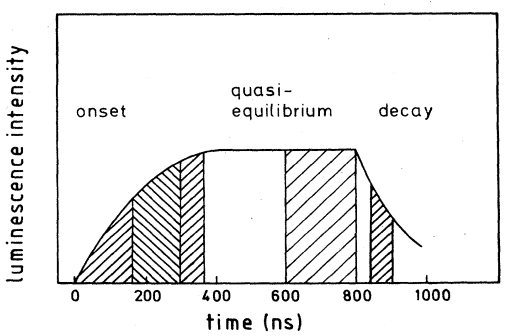

FIG. 3. Cathodoluminescence response to 800-ns electron pulse (schematically). Up to 14 time windows can be simultaneously set during onset, quasiequilibrium, and decay of the luminescence. A number of such windows is indicated by the differently hatched areas under the Cl curve.

if the system under investigation is not a two-level system, one initial and one final state, but more complex. Only a comparison of a number of time-delayed spectra, covering the entire wavelength range of interest, with the corresponding decay times, can, in general, lead to a physically meaningful interpretation. The cathodoluminescence system described here offers this possibility.

B. Crystals

All GaAs crystals used for the experiments described here were grown by liquid-phase epitaxy. The layers are either n or p type with net impurity concentrations of 1×10^{14}–1×10^{15} cm^{-3}. They are not intentionally doped, except for a few, which are lightly Sn doped. The thickness of all layers is larger than 20 μm, so that any influence of the substrate or its interface on the luminescence spectra can be disregarded.

III. THE ONSET OF LUMINESCENCE

The evolution of luminescence spectra of p-type samples excited with pulses of increasing length will be contrasted with the evolution of spectra of n-type samples at the beginning of this section. Then, capture times of holes into shallow effective-mass—acceptor states and into the 167-meV deep states of the Sn acceptor[10] are derived from the onset of acceptor-related luminescence. Finally, we demonstrate the strong dependence of the luminescence on the length of the exciting pulse.

Figure 4 shows typical luminescence spectra at 5.3 K of (a) a lightly-Sn-doped n-type sample and (b) a p-type sample. The spectra are taken *during* excitation with pulses of a length T increasing from 2 ns to 2 μs. The width of the time window during which photons are counted is typically 5% of the excitation pulse duration, but at least 2 ns. The counting window is always positioned at the end of the exciting pulse. For clarity, only three of these spectra are displayed here. An increase of the excitation pulse length beyond 500 ns does not lead to further changes of the spectra, for both n- and p-type samples. The spectra of both types of samples look qualitatively similar to those discussed in the detailed investigation of Heim and Heisinger.[23] Luminescence from the free exciton X, from the donor- and acceptor-bound excitons (D^0,X), (D^+,X), and (A^0,X), from the neutral-acceptor-tin-bound exciton (Sn^0,X),[24] from the free-electron—neutral-acceptor recombination (e,A^0), and from the neutral-donor—neutral-acceptor pair recombination (D^0,A^0) is easily identified.[14] The various lines are labeled at the top of Fig. 4.

Apparently, the spectral distribution of the emission depends on the length of the exciting pulse. The spectra after long excitation pulses show a larger variety of recombination processes than the spectra after short pulses. Following a 2-ns pulse the n-type sample does not show any features which are connected with the presence of neutral acceptors, whereas the p-type sample does not show any features connected with the presence of neutral donors. Thus, after excitation with pulses of 2 ns or shorter, recombination processes due to *bound* minority carriers are completely absent, although *free* minority car-

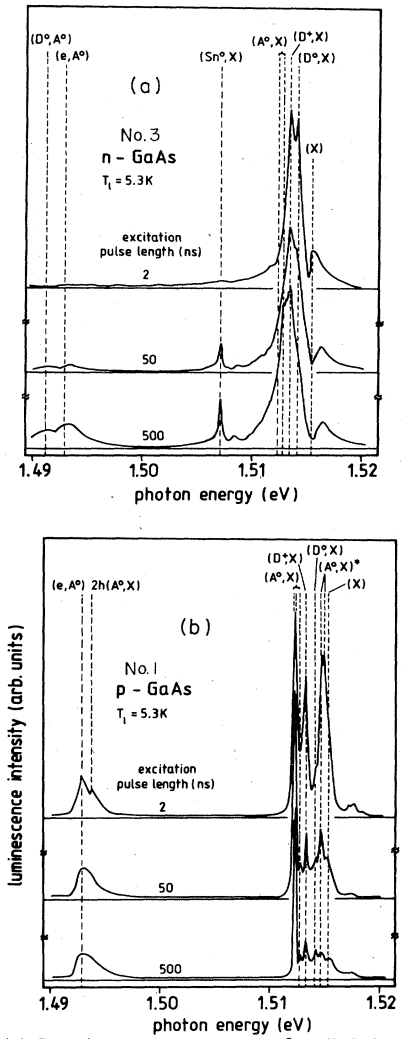

FIG. 4. (a) Luminescence spectra of a lightly-Sn-doped n-type sample, and (b) a high-purity p-type sample. The spectra shown here are taken during excitation with pulses of length 2, 50, and 500 ns, respectively.

riers are present. The capture of free minority carriers into bound states takes much longer than the time of excitation at the doping levels used here. These capture times will be derived in what follows. The spectra of Fig. 4 visualize directly for the first time the temporal evolution of the capture process of free minority carriers into shallow bound states in GaAs.

A brief remark shall be devoted to the lines at 1.5148 eV (500 ns) and 1.5150 eV (2 ns) which seems to exhibit some fine structure in the p-type sample and which are located just below the exciton band. These lines were tentatively assigned[23] to excited states of the neutral-donor bound exciton. The presence of an intense peak at times as short as 2 ns, the extreme weakness of the (D^0,X) line still at 500 ns, and its complete absence at 2 ns seem to exclude this interpretation. The energy difference of 2.5 meV to the (A^0,X) lines and the reciprocal time dependence of the (A^0,X) and 1.515-eV lines make it more likely that these lines are due to excited states of (A^0,X). An energy-relaxing cascade process via excited states apparently precedes the formation of the (A^0,X) ground state(s), in agreement with the early—but still valid—theory on cascade processes by Lax,[16] which was originally developed for donors. Very recently, Koteles *et al.*[25] interpreted the 1.515-eV line in p-type molecular-beam-epitaxy- (MBE-) grown samples as a free-exciton—polariton line. This interpretation does not seem to be consistent with the time evolution and doping dependence of the lines.

The excitation-pulse-length dependence of the luminescence spectra is used to evaluate capture times of free holes into acceptor ground states. Figure 5 shows the integrated luminescence intensity of the (Sn^0,X) line of Fig. 4(a) and of the (e,A^0) line in a different n-type sample which does not contain Sn or any other medium deep acceptor in a measurable concentration. With increasing time after the beginning of excitation, the relative intensities of both lines increase and eventually saturate [note the different time-scales in parts (a) and (b) of the figure].

The intensity $\{I(t)\}_{(Sn^0,X)}$ (photons/s) of the (Sn^0,X) recombination at a time t after the start of a continuous pulse is

$$\{I(t)\}_{(Sn^0,X)} \sim \frac{[Sn^0,X]_t - [Sn^0,X]_0}{\tau_t}\eta V , \tag{1}$$

where the concentration of excitons bound to the neutral-acceptor tin in thermal equilibrium $[Sn^0,X]_0=0$, since in an n-type material at low temperatures the neutral-acceptor-tin concentration $[Sn^0]=0$. τ_t is the total lifetime of the bound exciton, η is the internal quantum efficiency, and V is the volume. Since V and η are to a first approximation time independent, Eq. (1) can be simplified to

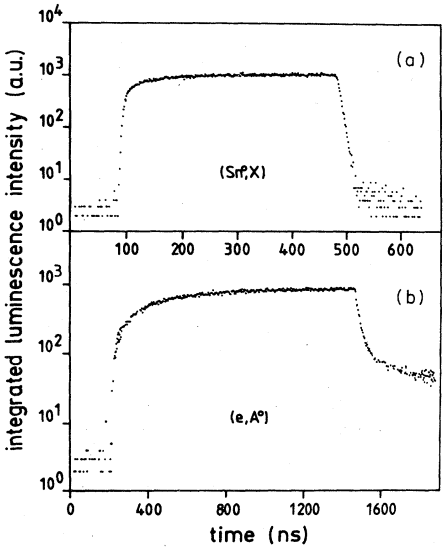

FIG. 5. Time dependence of luminescence intensity of the (a) (Sn^0,X) and (b) (e,A^0) luminescence in a Sn-doped and a nominally undoped n-type sample, respectively. A^0 is the effective-mass acceptor carbon.

$$\{I(t)\}_{(\mathrm{Sn}^0,X)} \sim \frac{[\mathrm{Sn}^0,X]_t}{\tau_t} . \tag{2}$$

Now,

$$[\mathrm{Sn}^0,X]_t \sim [\mathrm{Sn}^0]_t[X]_t , \tag{3}$$

where $[X]$ is the concentration of excitons.

Figure 4 shows that the free-exciton concentration $[X]$ is close to being time independent on the ns timescale, which is relevant here. Already at 2 ns we observe a strong free-exciton peak but no sign of the tin bound exciton. Obviously the creation of free excitons from free charge carriers is much faster. Ulbrich[26] found under somewhat different experimental conditions a free-exciton creation time of 0.3 ns. Thus the time dependence of $[\mathrm{Sn}^0,X]$ is governed by the time dependence of $[\mathrm{Sn}^0]$:

$$\mathrm{Sn}^- + h \rightarrow \mathrm{Sn}^0 . \tag{4}$$

The reaction equation (4) represents the capture of free holes by ionized Sn acceptors, with

$$[\mathrm{Sn}^0]_t = [\mathrm{Sn}^-][1-\exp(-t/\tau_c)] , \tag{5}$$

where τ_c is the hole-capture time.

Combining Eqs. (2), (3), and (5) we obtain

$$I(t) \sim [\mathrm{Sn}^-][1-\exp(-t/\tau_c)]\tau_t . \tag{6}$$

A more detailed calculation shows that

$$I(t) \sim [\mathrm{Sn}^-]\exp(-\tau_c/\tau_t)[1-\exp(-t/\tau_c)] . \tag{7}$$

The experimental data of Fig. 5(a) can be perfectly fitted using Eq. (7) with $\tau_c = 7 \pm 1$ ns, the time to capture a hole by an ionized tin acceptor. Using

$$\tau_c = (\sigma_p \hat{v}_{\mathrm{th}}[\mathrm{Sn}^-])^{-1} , \tag{8}$$

an estimate of the hole capture cross section σ_p of tin can be made. $N_D - N_A$ of the particular Sn-doped sample of Fig. 5(a) was 4.6×10^{14} cm^{-3} at 77 K and 5.2×10^{14} cm^{-3} at 300 K. We assume that Sn is the dominant donor—the residual donor concentration in nominally undoped samples grown under similar conditions is much lower. Tin is an amphoteric impurity with $[\mathrm{Sn_{Ga}}]/[\mathrm{Sn_{As}}] \simeq 14$.[27] From the 77-K mobility value of 78 100 cm^2/V s, we obtain, in conjunction with Fig. 3 of Ref. 28 for the total donor concentration, $[D] = 8.7\times10^{14}$ cm^{-3}, and for the total acceptor concentration, $[A] = 3.5\times10^{14}$ cm^{-3}. Then, $[\mathrm{Sn_{Ga}}] = 8.7\times10^{14}$ cm^{-3} and $[\mathrm{Sn_{As}^-}] = 6.2\times10^{13}$ cm^{-3}. We assume further that the mean temperature of the holes is 15 K,[29] and that their kinetic mass is equal to the mean heavy-hole mass $m_h = 0.64 m_0$.[30] Then, $\hat{v}_{\mathrm{th}} = (3kT/m_h)^{1/2} = 3.3\times10^{16}$ cm/s. Thus the hole capture cross section of Sn is found to be

$$\sigma_p(\mathrm{Sn}) \cong 7.0\times10^{-13} \text{ cm}^2 , \tag{9}$$

in qualitative agreement with the values found for other hole traps in GaAs by DLTS.[14] The precision of σ_p(Sn) certainly could be improved by a direct quantitative determination of the total tin concentration of the sample.

Similar arguments as above can be used to describe theoretically the excitation time dependence of the (e,A^0) luminescence intensity shown in Fig. 5(b). A capture time of the hole into the shallow, effective-mass-like acceptor of 12 ns is found. The energetic position[14] and shape of the spectrum clearly show that there is only one dominant shallow acceptor present: carbon. The carbon concentration is 2.9×10^{14} cm^{-3}. Thus the hole capture cross section of carbon is

$$\sigma_p(\mathrm{C}) \approx 8.7\times10^{-14} \text{ cm}^2 . \tag{10}$$

The transients of the luminescence after the end of the exciting pulse change in a still more striking way than the spectra upon variation of excitation pulse length. Figure 6 shows the integrated luminescence intensity of the n-type sample of Fig. 4 as a function of time after excitation by pulses of 2, 50, and 500 ns duration. The transients obviously *depend strongly on the pulse length, as long as a quasi-steady-state is not reached.* The transients *do not vary any farther* for excitation pulse lengths longer than 1 μs.

At a pulse length of 2 ns the intensity decays with a time constant $\cong 1$ ns. A comparison with the spectra of Fig. 4(a) proves that this is the decay time of the donor bound excitons (D^0,X) and (D^+,X), in excellent agreement with the values 1.07 and 0.8 ns, respectively, found by Hwang.[31] These times are the true lifetimes of the bound excitons and not the capture times of free excitons and/or free electrons and holes by donors. The capture time varies inversely with trap density [see Eq. (8)], and for different samples with different donor concentrations different decay times would be expected.

The presence of strong bound-exciton luminescence after excitation with (1—2)-ns pulses and its instantaneous increase (on this timescale) upon excitation also proves independently that the bound-exciton creation via exciton capture must be much faster, in contrast to Hwang's assumption.[31] Using pulses of increasing length the transients are increasingly influenced by the decay of the neutral minority centers—the acceptors—via the (e,A^0), (D^0,A^0), and (A^0,X) decay channels. The fast decay time

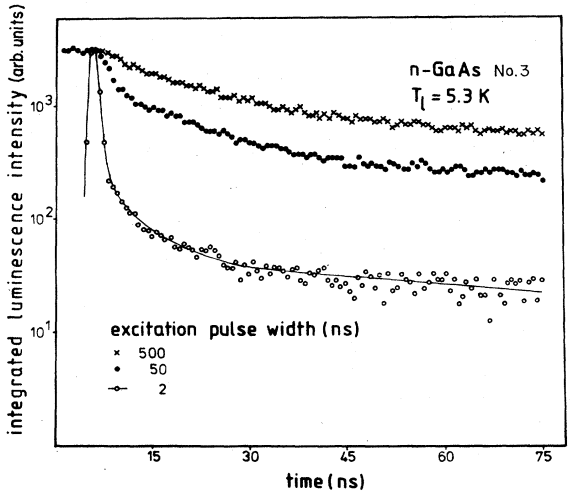

FIG. 6. Transients of the integrated luminescence intensity of sample 3 of Fig. 4(a) for excitation pulse widths of 2, 50, and 500 ns.

after 500-ns excitation, $\tau_1 = 8$ ns, found here, cannot be understood on the basis of the results presented so far. More results leading to a consistent interpretation will be presented in Sec. IV A. The very slow decay at long times after the end of excitation is due to slow (e,A^0) and (D^0,A^0) recombination processes which will be discussed in detail in the next section.

IV. THE DECAY FROM QUASIEQUILIBRIUM

In the preceding section we showed that a meaningful interpretation of luminescence transients is at least difficult if not altogether prevented if the influence of the pulse length on the relative population of the various excited states is not taken into account. Short pulse transients cannot be compared to or interpreted on the basis of cw spectra. In this section spectra are reported which are taken at various delay times after the end of a long pulse with a typical length of 2 μs. The variation of the luminescence intensity of different recombination processes with time is investigated. Capture and recombination time constants of free electrons and holes are derived. Figure 7 shows, on a semilogarithmic scale, time-delayed spectra of a p-type sample taken at delay times of 0, 20, and 50 ns after excitation, with a spectral resolution of 0.1 nm. The width of the time window is 10 ns and the excitation density is 6 W/cm^2. At 0 ns delay the near-band-edge luminescence (bound excitons and exciton X) is slightly stronger than the neutral-acceptor—free- or bound-electron recombination between 1.49 and 1.50 eV. The linear high-energy tails of the (e,A^0) and X bands are indicative of Maxwellian distributions of electrons and excitons. The temperatures of these distributions can be directly derived from Fig. 7 as a function of delay time. Detailed information on warm electron—acoustic-phonon interaction and the screening of this interaction is obtained. This information is discussed separately.[21,29] However, it should be noted here that electrons and excitons, and thus also holes, have the same temperature (different from lattice temperature), as can be seen directly from Fig. 7, in contrast to earlier assumptions.[32]

With increasing time after the end of excitation, the near-band-gap luminescence rapidly decreases, whereas the (e,A^0) and (D^0,A^0) bands gain relatively in intensity. At times as short as 20 ns after excitation, the band (e,A^0) completely dominates the spectrum. Later, the pair band appears and becomes quite prominent with increasing delay time. These qualitative changes of the spectra are independent of excitation intensity.

Further insight is gained by monitoring the transients of the spectra. In Fig. 8 the transients of the integrated luminescence of the near band edge and of the sum of $(e,A^0)+(D^0,A^0)$ luminescence are shown. The excitation intensity here is 20 W/cm^2. The near-band-edge luminescence decays approximately 1 order of magnitude faster than the luminescence at longer wavelengths. During the first few ns the decay of the integrated luminescence is dominated by these fast processes, then the transients display the much slower decay of the $(e,A^0)+(D^0,A^0)$ recombination.

A first qualitative conclusion can be immediately drawn based upon Figs. 7 and 8. 50 ns after the excitation is switched off, free electrons are still present, as is proved unambiguously by the dominance of the (e,A^0) recombination line in the spectra. The excitonic lines, however, have more or less disappeared. Consequently, free holes are not present any more and the conductivity type is inverted from p to n. At first sight, this result is quite surprising, since it is deduced from experiments on p-type samples. One might expect that the minority carriers, the electrons, disappear first. At temperatures as low as 5 K, however, almost no free holes exist in thermal equilibrium due to the comparatively large effective-mass acceptor binding energy. Capture cross sections of ionized acceptors are found to be much larger than those of donors. Thus free holes are captured by ionized acceptors before

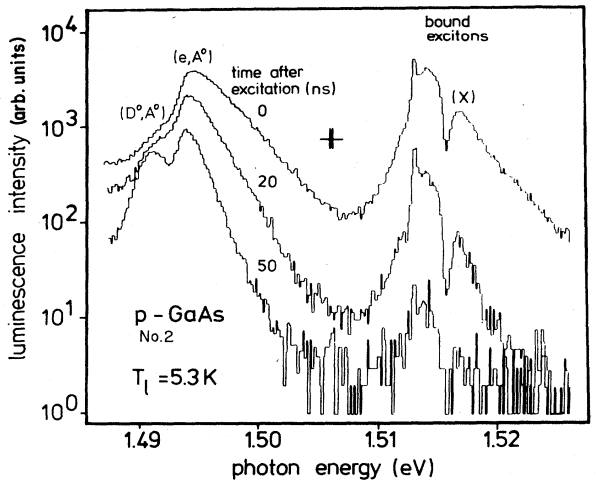

FIG. 7. Time-delayed spectra of a p-type sample taken after the end of a 2-μs excitation pulse.

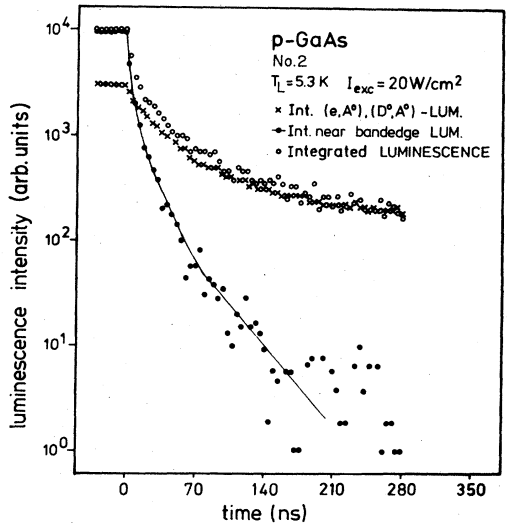

FIG. 8. Comparison of the transients of the integrated luminescence, the near-band-edge luminescence, and the $(e,A^0)+(D^0,A^0)$ luminescence after the end of a 2-μs excitation pulse.

electrons are captured by ionized donors in n- and p-type material as long as both types of ionized impurities are present at not too different concentrations ($N_{A^-} \cong N_{D^+}$). The actual capture times depend, of course, on the values of N_{A^-} and N_{D^+} [see Eq. (8)].

A. Free hole to effective-mass acceptor capture times and cross sections

The time dependence of the near-band-edge spectra after the end of excitation is now investigated and discussed in more detail. The lifetime of free holes and the capture cross section of free holes by effective-mass acceptors is determined. It is found that the excited electronic states of the crystal relax in small steps via intermediate states such as free excitons and bound-exciton excited states. Figure 9 shows on an extended energy scale the near-band-edge spectra for a p-type sample at delay times of 0, 8, 16, and 25 ns. The identification of the rather well-resolved lines, (A^0,X), (D^+,X), (D^0,X), $(A^0,X)^*$, free exciton X, and donor excited state (D^{0*},h), is given at the top of Fig. 9. The excitation intensity here is 1 W/cm^2. At 0 ns delay time the system starts to decay from a quasiequilibrium state. Approximately 40% of the total luminescence intensity of this group of lines is due to the bound excitons (A^0,X) and (D^+,X), whereas the radiative decay of the free exciton and of the excited state $(A^0,X)^*$ accounts for 60% of the light intensity. With increasing time this ratio changes and, at long delay times, (A^0,X) and (D^+,X) contribute relatively more to the emission intensity. The intensity ratio $I((A^0,X))/I((D^+,X))$ is found to be time independent.

The pronounced relative weakening with increasing delay time of X as compared to (A^0,X) is expected on the basis of what was already stated above: free holes disappear more rapidly than free electrons, thus inhibiting regeneration of free excitons. Neutral acceptors and ionized donors—which are both present in thermal equilibrium and which are the final states of the (A^0,X) and (D^+,X) recombinations—on the other hand, quickly recapture excitons. The neutral-acceptor bound-exciton excited state $(A^0,X)^*$ apparently acts as an efficient intermediate state in the series of steps of relaxation and capture processes. With increasing time $(A^0,X)^*$ relaxes to the ground state (A^0,X). This emission-recapture circular process is sustained as long as holes exist. Thus the ultimate decay of the entire ensemble of lines is governed by the hole lifetime. Both additional time constants of relevance here, the capture time of excitons by impurities and the bound-exciton lifetime(s), are much shorter, as found in Sec. III. This conjecture is verified by a detailed investigation of the transients. Figure 10 shows the time dependence of a spectral window of 0.2 meV centered at 1.512 eV—the spectral position of (A^0,X)— at three different excitation intensities. Here, $I_0=20$ W/cm^2. Two different decay times are apparently superimposed. A rapid decay with $\tau_1=10$ ns is followed by a much slower one with $\tau_2=52$ ns. The time constant τ_1 is given by the capture of free holes. There are at least two competing capture processes which contribute: (a) capture of holes by ionized acceptors, and (b) capture of holes by electrons (formation of excitons). The latter process will be first excluded. It is a bimolecular one. If it dominated the decay, the time dependence of the luminescence intensity should be nonexponential as long as the number of externally excited holes was larger than the thermal equilibrium number. Figure 10 clearly shows—in particular, at the highest excitation intensity I_0—that the initial decay is exponential (for a range of I_0 over 2 orders of magnitude). We thus

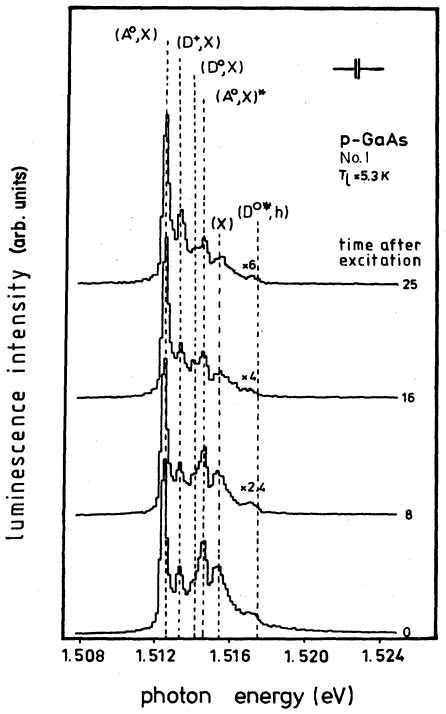

FIG. 9. Detailed time-delayed spectra of near-band-edge luminescence of a high-purity p-type sample after excitation with a 2-μs pulse. The lines are slightly broadened due to the finite channel width of the data-acquisition system.

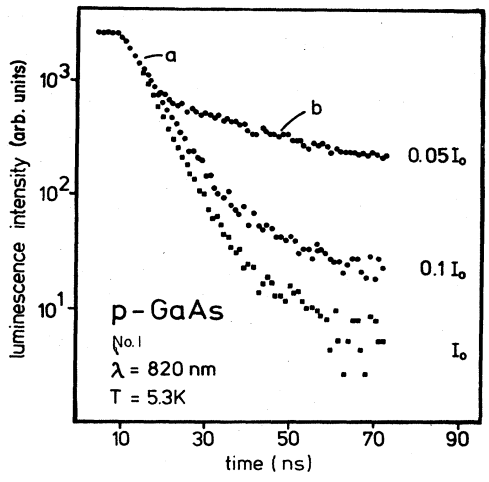

FIG. 10. Transients of the (A^0,X) recombination at three different excitation intensities. $I_0=20$ W/cm^2.

conclude that the time constant τ_1 is dominated by the capture of holes by ionized (carbon) acceptors. From a theoretical point of view this process is also expected to have a much larger cross section than the free-exciton formation.

At a first sight, it is somewhat surprising that at longer times another—longer—time constant τ_2 starts to dominate the decay. This time constant is again independent of the initial excitation conditions, as can be clearly seen from Fig. 10. As long as free electrons are present and as long as the hole temperature T_h is larger than the lattice temperature, the total capture rate of holes is slightly larger than the thermal reemission rate of holes from neutral acceptors. Thermal reexcitation of holes from bound states leads to a preservation of bound-excitonic recombination processes at a low and permanently decreasing level as long as free electrons are present.

The capture cross section of the carbon acceptor, the only acceptor present in the spectrum of sample no. 1, can be deduced from τ_1 using Eq. (8). The acceptor concentration of this sample is 3×10^{14} cm^{-3}. Using again a temperature of the holes of 15 K and $m_h=0.64m_0$,

$$\sigma_p(\mathrm{C})=10.1\times10^{-14}\ \mathrm{cm}^2\ , \tag{11}$$

in good agreement with the value derived independently in Sec. III from an n-type sample.

The transients of the near-band-edge spectra of a number of n- and p-type samples are investigated in this way and under identical conditions. Figure 11 compares the results of two more samples, an n-type sample doped with tin and another p-type sample having a somewhat larger acceptor concentration than sample no. 1. Table I summarizes the decay times of the near-band-edge spectra of all samples for which spectra are presented here. The hole lifetime of sample no. 2 is 3.5 ns. Assuming a similar background donor concentration as in sample no. 1, we obtain $N_A=1.2\times10^{15}$ cm^{-3} and

$$\sigma_p(\mathrm{C})=7.2\times10^{-14}\ \mathrm{cm}^2\ . \tag{12}$$

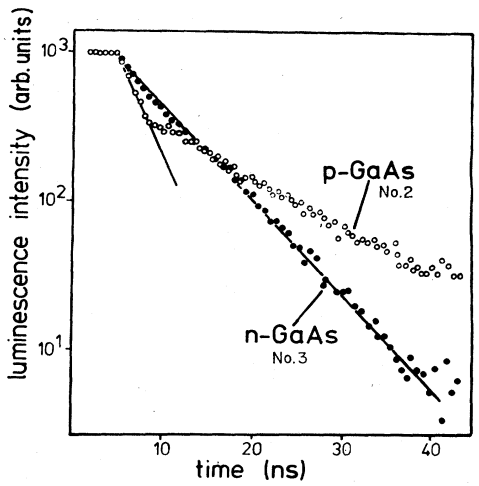

FIG. 11. Comparison of the transients of the near-band-edge spectra of an n- and a p-type sample.

The smallness of the difference between the three values obtained for σ_p(C) here and in Sec. III is proof of the reliability of our results and of the method. We find, for the mean value,

$$\sigma_p(\mathrm{C})=(8.7\pm2)\times10^{-14}\ \mathrm{cm}^2\ . \tag{13}$$

The error is estimated from the uncertainty in the determination of the true acceptor concentration, and there is no obstacle to reducing this error in future experiments. To the best of our knowledge this is the first time that the hole capture cross section of an effective-mass acceptor in GaAs has been determined.

B. Free-electron recombination

The valence-band excess population decays more rapidly than the conduction-band excess population for all

TABLE I. Summary of capture times and capture cross sections of the different processes investigated here.

Capture process	Type of experiment	Sample no.	Capture time (ns)	Sample properties: Conductivity type	Sample properties: Majority impurity concentration (cm^3)	Capture cross section (cm^2)
1 (h,C$^-$)	Onset of (e,C^0)	3	12±3	n	2.9×10^{14}	8.7×10^{-14}
2 (h,C$^-$)	Decay of near-band-gap lines	1	10±1	p	3×10^{14}	10.1×10^{-14}
3 (h,C$^-$)	Decay of near-band-gap lines	2	3.5±0.5	p	1.2×10^{15}	7.2×10^{-14}
4 (h,Sn$^-$)	Onset of (Sn^0,X)	3	7±1	n	6.2×10^{13}	7×10^{-13}
5 (e,D^+)	Decay of (e,C^0)	3	22±2	n	8.7×10^{14}	5.1×10^{-15}
6 (e,C^0)	Decay of (e,C^0)	3	2500±500	n	3.5×10^{14}	1.8×10^{-16}

samples investigated, after the end of external excitation, independent of doping type, temperature, and excitation intensity. Three recombination processes of free and bound electrons eventually reestablish thermal equilibrium:

(1) Capture of free electrons by ionized donors.
(2) Capture of free electrons by neutral acceptors.
(3) Recombination of electrons bound to donors with holes bound to acceptors (pair recombination).

Processes (1) and (2) compete to reduce the free-electron density. Time-delayed spectra let us conclude that process (1) is by far the faster, in agreement with theoretical predictions.[16–18] Figures 12 and 13 show the (e,A^0) and (D^0,A^0) recombination lines of an n- and p-type sample 0—540 ns after excitation at different temperatures. One feature is typical for the spectra of both types of samples: At short delay times the pair-band intensity shows a strong relative increase with time. Then, after 150—250 ns this process reverses and (e,A^0) grows slowly with time as compared to (D^0,A^0). The rapid relative increase of (D^0,A^0) at delay times up to ≈ 150 ns is due to a relative increase of the number of electrons bound to donors as compared to free electrons. This relative increase is, of course, more pronounced in a p-type sample, which contains no neutral donors in thermal equilibrium, than in an n-type sample. The process saturates after the thermal population ratio,

$$N_f/N_b = g\exp(-E_T/kT_l)\ , \tag{14}$$

has been reached. N_f and N_b are the numbers of electrons in free and bound states, respectively, g is the density of states ratio, E_T is the thermal activation energy of the donor, and T_l is the lattice temperature.

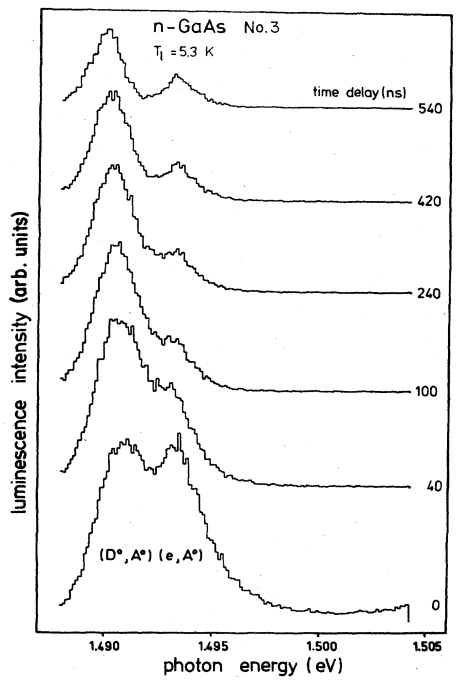

FIG. 12. Time-delayed spectra of (e,A^0) and (D^0,A^0) recombination in an n-type sample at 5.3 K after the end of a 2-μs excitation pulse.

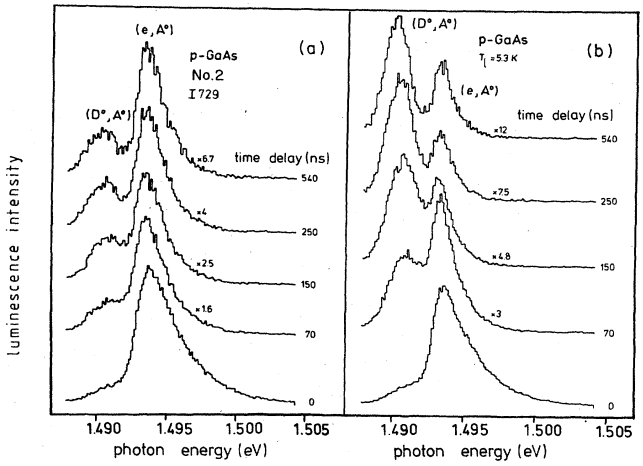

FIG. 13. Time-delayed spectra of (e,A^0) and (D^0,A^0) recombination at (a) 13 K and (b) 5.3 K in a p-type sample after the end of a 2-μs excitation pulse.

At still larger delay times one might expect that both recombination bands would disappear synchronously since the relative occupation ratio N_f/N_b will remain constant until the end of the recombination if T_l does not change. Since the (e,A^0) recombination rate is larger than the (D^0,A^0) recombination rate,[33,34] the thermal population ratio is distorted and electrons must be permanently reexcited from donor sites to the conduction band to reestablish the thermal population. With increasing time the total number of neutral acceptors and donors is reduced and the mean distance R between recombining pairs is increased. As a consequence, the mean photon energy of the pair band,[33,34]

$$\hbar\omega = E_g - E_D - E_A + e^2/\epsilon R\ , \tag{15}$$

decreases. E_D and E_A are the donor and acceptor binding energies, respectively. This red shift of the peak and the synchronous disappearance of the high-energy tail of the pair band is nicely visualized in Figs. 12 and 13. With increasing distance R of the pairs, also the radiative recombination probability is exponentially reduced:

$$W_{DA}(R) = W_{DA}^0\exp(-2R/a_D)\ , \tag{16}$$

where a_D is the Bohr radius of the donor. On the other hand, the recombination probability of (e,A^0) is not affected by the decreasing number of free carriers, as far as many-particle effects can be neglected. Thus at delay times larger than 150 ns the intensity ratio $I((D^0,A^0))/I((e,A^0))$ decreases although the population ratio N_f/N_b remains constant.

After a qualitative understanding of the processes governing the free- and bound-electron recombination at long delay times has been reached, we shall now derive capture cross sections for the capture of electrons by ionized donors and neutral acceptors. Figure 14 shows the transient of the integrated (e,A^0) intensity of sample no. 3

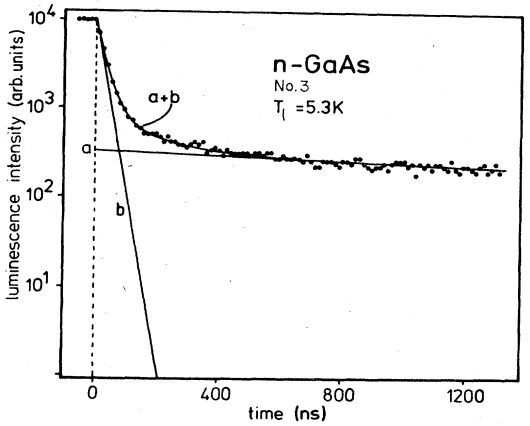

FIG. 14. Transient of the integral (e,A^0) luminescence intensity of sample 3 (see Fig. 12) after the end of a 2-μs excitation pulse.

(see Fig. 12 for comparison). The range of integration covers the entire (e,A^0) luminescence region.

The experimental points of Fig. 14 are well approximated by a sum of two exponential decays with different weights, as shown by the straight lines in the figure. Decay times of $\tau_1=22.5\pm2$ ns and of $\tau_2=2.5\pm0.5$ μs are found, in qualitative agreement with decay experiments under impact-ionization conditions by Bludau and Wagner.[35] τ_1 is the electron$\rightarrow$ionized-donor capture time. Assuming—as in Sec. III—a donor concentration $N_D=8.7\times10^{14}$ cm^3, a mean electron temperature of 15 K, and an electron mass $m_e=0.0665m_0$, we obtain $\hat{v}_{\rm th}=(3kT/m_e)^{1/2}=1\times10^7$ cm/s. The capture cross section of the tin donor is therefore

$$\sigma_{(e,D^+)}({\rm Sn})=(5.1\pm1.1)\times10^{-15}\ {\rm cm}^2\ . \tag{17}$$

Similarly, the capture cross section of electrons by neutral effective-mass acceptors is derived from τ_2, which is the electron$\rightarrow$neutral-acceptor capture (recombination) time, using $N_A=3.5\times10^{14}$ cm^{-3}. A value

$$\sigma_{(e,A^0)}=(1.8\pm0.5)\times10^{-16}\ {\rm cm}^2 \tag{18}$$

results. A temperature of 6 K and a thermal velocity of 0.64×10^7 cm/s is used here. The systematic error of $\sigma_{(e,A^0)}$ is somewhat larger than that of $\sigma_{(e,D^+)}$ for a number of reasons. The acceptor concentration is estimated with less precision than the donor concentration. The decay time of (e,A^0) is influenced by the decay rate of the pair band, which decays nonexponentially due to the R dependence mentioned above. Since the free-electron states are more rapidly depleted than the bound-electron ones, but N_f/N_b remains constant, permanently free carriers are reexcited, leading to a reduced decrease of the free-carrier generation and to a somewhat increased "decay time." Finally, the sample also contains a small concentration of [Sn_{As}], another acceptor. Its influence is most probably negligible since $\tau_{(e,A^0)}\sim E_A^3$.[18]

Using the 15-μs lifetime of the (e,A^0) transition found by Bludau and Wagner[35] in a sample with a smaller but less precisely known acceptor concentration, we calculate $\sigma_{(e,A^0)}\approx2\times10^{-16}$ cm^2, in excellent agreement with the above results. Table I summarizes and compares the capture cross sections determined in Secs. III and IV of this paper together with the relevant experimental parameters.

V. CONCLUSION

The kinetics of capture and recombination processes of nonequilibrium electrons and holes in high-purity n- and p-type GaAs are investigated in detail in a specially devised low-temperature cathodoluminescence system. The fundamentals of the kinetics of relaxation and capture in a direct-band-gap semiconductor are revealed for the first time and the first determination of a number of capture cross sections is presented.

Impurity-induced recombination paths are known to be the dominant ones at low temperatures in zinc-blende semiconductors. After excitation with pulses of a few ns length, however, only centers which were present in thermal equilibrium before excitation are found to contribute to the recombination. These are, in p-type material, neutral and ionized acceptors and ionized donors, but not neutral donors; and in n-type material, neutral and ionized donors and ionized acceptors, but no neutral acceptors. With increasing length of excitation the character of the luminescence is found to change since minority centers increasingly capture charge carriers and are neutralized. Emission from a quasiequilibrium excited state is found to occur only after long times of the order of 1 μs. Cross sections of capture of holes by the ionized effective-mass acceptor carbon ($E_A=26$ meV) and by the ionized acceptor tin ($E_A=167$ meV) are determined from the onset of the corresponding luminescence in n-type samples. These cross sections are $\tau(h\rightarrow C^-)=8.7\times10^{-14}$ cm^2 and $\tau(h\rightarrow Sn_{As}^-)=7.0\times10^{-13}$ cm^2.

Time-delayed spectra and luminescence transients taken after the end of 2-μs-long exciting pulses display in great detail the stepwise return to thermal equilibrium from the quasiequilibrium excited state. The rapid intensity decrease of the near-band-gap emission which is observed in n- and p-type samples is caused by the rapid capture of free holes by ionized acceptors. Nonequilibrium holes recombine or are captured much faster than nonequilibrium electrons independent of the conductivity type of the material, since hole capture cross sections are orders of magnitude larger, as seen in Table I. Capture cross sections of holes by the ionized effective-mass acceptor carbon are determined from the decay of the near-band-gap emission for various p-type samples and found to agree well with the cross sections determined from n-type samples.

At long times after excitation, the final steps of the return to equilibrium involve only free and shallow donor-bound electrons, and holes bound to acceptors. Cross sections of capture of free electrons by ionized effective-mass donors and by neutral acceptors are derived from the transients of the (e,A^0) recombination. These cross sections

are $\tau(e \rightarrow D^+) = 5.1 \times 10^{-15}$ cm^2 and $\tau(e \rightarrow A^0) = 2 \times 10^{-16}$ cm^2 (A^0=carbon here). The $e \rightarrow A^0$ capture (recombination) is found to be the weakest by far of all processes investigated. However, its cross section is still 2 orders of magnitude larger than the cross section τ_{nr} for nonradiative deep-level capture measured by Lang and Henry.[36] Bulk recombination in GaAs is predominantly radiative.

Our data provide for the first time a reasonable basis for comparison with advanced theories of capture cross sections which should in the future take into account the correct valence-band structure and acceptor wave functions of zinc-blende semiconductors.

ACKNOWLEDGMENTS

Parts of this work which were performed during the author's stay at the Institut für Halbleitertechnik Aachen were funded by the Deutsche Forschungsgemeinschaft. We are indebted to E. Schöll for helpful discussions in the initial stage of this work and to M. S. Skolnick for a critical reading of the manuscript. E. Bauser and K. H. Zschauer grew the excellent layers used here.

[1]H. Bebb and R. A. Chapman, J. Phys. Chem. Solids **28**, 2087 (1967).
[2]G. Lucovsky, Solid State Commun. **3**, 299 (1965).
[3]S. T. Pantelides, Rev. Mod. Phys. **50**, 797 (1978).
[4]H. Bebb, Phys. Rev. **185**, 1116 (1969).
[5]B. K. Ridley, J. Phys. C **13**, 2015 (1980).
[6]S. Chaudhuri, Phys. Rev. B **26**, 6593 (1982).
[7]A. Baldereschi and N. O. Lipari, Phys. Rev. B **8**, 2697 (1973); **9**, 1525 (1974).
[8]N. O. Lipari and A. Baldereschi, Solid State Commun. **25**, 665 (1978); N. O. Lipari, Phys. Lett. **81A**, 75 (1981).
[9]D. Bimberg and A. Baldereschi, in *Proceedings of the 14th International Conference on the Physics of Semiconductors, Edinburgh (1978),* edited by B. L. H. Wilson (IOP, Bristol, 1979), p. 403 (Inst. Phys. Conf. Ser. No. 43); D. Bimberg, Phys. Rev. B **18**, 1794 (1978).
[10]W. Shairer, D. Bimberg, W. Kottler, K. Cho, and M. Schmidt, Phys. Rev. B **13**, 3452 (1976).
[11]D. V. Lang, J. Appl. Phys. **45**, 2023 (1974); G. L. Miller, D. V. Lang, and L. C. Kimmerling, Ann. Rev. Mater. Sci. **7**, 377 (1977); H. G. Grimmeiss, E. Janzén, and B. Skarstam, J. Appl. Phys. **51**, 3740 (1980).
[12]For example, A. Chantre, G. Vincent, and D. Bois, Phys. Rev. B **23**, 5335 (1981); H. Lefèvre and M. Schulz, Appl. Phys. **12**, 45 (1977); IEEE Trans. Electron. Dev. **ED-24**, 973 (1977).
[13]S. Makram-Ebeid, Appl. Phys. Lett. **37**, 464 (1980); S. Makram-Ebeid, G. M. Martin, and D. W. Woodard, J. Phys. Soc. Jpn. Suppl. A **49**, 287 (1980); S. Makram-Ebeid and M. Lannoo, Phys. Rev. Lett. **48**, 1281 (1982).
[14]*Landolt-Börnstein,* New Series, edited by O. Madelung (Springer, Heidelberg, 1982), Group III, Vol. 17a.
[15]U. Heim, in *Advances in Solid State Physics XII,* edited by O. Madelung (Teubner, Wiesbaden, FRG, 1972), p. 183.
[16]M. Lax, Phys. Rev. **119**, 1502 (1960).
[17]D. R. Hamann and A. L. McWhorter, Phys. Rev. **134**, 250 (1964).
[18]W. P. Dumke, Phys. Rev. **132**, 1998 (1963).
[19]A. Steckenborn, H. Münzel, and D. Bimberg, J. Lumin. **24-25**, 351 (1981); in *Proceedings of the Microscopic Semiconducting Materials Conference, Oxford,* edited by P. Hirsch (IOP, Bristol, 1981), p. 185 (IOP Conf. Proc. Ser. No. 60).
[20]A. Steckenborn, H. Münzel, and D. Bimberg, Beitr. Elektronenmikroskop. Direktabb. Oberfl. **13**, 157 (1980).
[21]H. Münzel, D. Bimberg, and A. Steckenborn, Physica (Utrecht) **117&118B**, 214 (1983), and unpublished.
[22]M. Boulou and D. Bois, J. Appl. Phys. **48**, 4713 (1977).
[23]U. Heim and P. Hiesinger, Phys. Status Solidi B **66**, 461 (1974).
[24]D. Bimberg, W. Schairer, M. Sondergeld, and T. O. Yep, J. Lumin. **3**, 175 (1970).
[25]E. S. Koteles, J. P. Salerno, W. Bloss and E. M. Brody, in Proceedings of the 17th International Conference on the Physics of Semiconductors (unpublished).
[26]R. Ulbrich, Ph.D. thesis, University of Frankfurt, 1972.
[27]M. Maier, B. Hanel, and P. Balk, J. Appl. Phys. **52**, 342 (1981).
[28]D. L. Rode and S. Knight, Phys. Rev. B **3**, 2534 (1971).
[29]D. Bimberg, H. Münzel, and A. Steckenborn, J. Phys. (Paris) Colloq. **42**, C7-137 (1981); H. Münzel, A. Steckenborn, and D Bimberg, J. Lumin. **24-25**, 569 (1981).
[30]D. Bimberg, in *Festkörprobleme (Advances in Solid State Physics),* edited by J. Treusch (Vieweg, Braunschweig, 1977), Vol. XVII, p. 195.
[31]C. J. Hwang, Phys. Rev. B **8**, 646 (1973).
[32]R. Ulbrich, Phys. Rev. B **8**, 5119 (1973); Solid State Electron. **21**, 51 (1978).
[33]H. B. Bebb and E. W. Williams, in *Semiconductors and Semimetals 8,* edited by R. K. Willardson and A. C. Beer (Academic, New York, 1972), p. 182.
[34]G. H. Doehler, Phys. Status Solidi B **45**, 705 (1971).
[35]W. Bludau and E. Wagner, Appl. Phys. Lett. **29**, 204 (1976).
[36]D. V. Lang and C. H. Henry, Phys. Rev. Lett. **35**, 1525 (1975).